

## Conference Paper

# Sodium-23 Magnetic Resonance Imaging

Sadykhov E.G.<sup>1</sup>, Gulyaev M.V.<sup>2</sup>, Anisimov N.V.<sup>2</sup>, Pirogov Yu.A.<sup>2</sup>,  
and Belyaev V.N.<sup>1</sup>

<sup>1</sup>National Research Nuclear University MEPhI (Moscow Engineering Physics Institute),  
Kashirskoe shosse 31, Moscow, 115409, Russia

<sup>2</sup>Lomonosov Moscow State University, Moscow, Russia

## Abstract

<sup>23</sup>Na MRI provides additional biochemical information to <sup>1</sup>H MRI in terms of cell integrity and tissue viability. We aimed at determining the sensitivity of <sup>23</sup>Na MRS, MRI and MR relaxometry methods available on 7T MR scanner Bruker Biospec 70/30 USR and developing of an optimal MRI protocol for small animal <sup>23</sup>Na *in vivo* visualization. The outcomes include <sup>23</sup>Na MR spectra, <sup>23</sup>Na MR images with SNRs, and T<sub>1</sub> and T<sub>2</sub> values of <sup>23</sup>Na. It is shown that single-pulse <sup>23</sup>Na MR spectroscopy can discriminate different <sup>23</sup>Na concentrations, and 3D FLASH pulse sequence adapted for <sup>23</sup>Na data acquisition may provide the acceptable quality images.

**Keywords:** Sodium MRI, Sodium MRS, 3D FLASH, MR relaxometry

## 1. Introduction

Sodium is a vital component in the human organism. It is an important electrolyte that helps maintain the homeostasis of the organism through the osmo- and pH-regulation [1]. Sodium is a crucial element in cell physiology, which regulates the transmembrane electrochemical gradient and so participates in heart activity, the transmission of nerve impulses and muscle contractions. Sodium concentration (intracellular 10–15 mM and extracellular 140–150 mM) is very sensitive to changes in tissue metabolic state and to disruption of cell membrane integrity. In many pathological states, the sodium concentration increase is detected.

The sodium flux in and out of cells may occur by different mechanisms: voltage- and ligand-gated Na<sup>+</sup> channels, Na<sup>+</sup>/Ca<sup>2+</sup> exchangers, Na<sup>+</sup>/H<sup>+</sup> exchangers, Na<sup>+</sup>/HCO<sub>3</sub><sup>-</sup> cotransporters, Na<sup>+</sup>/K<sup>+</sup>/2Cl<sup>-</sup> cotransporters, Na<sup>+</sup>/Mg<sup>+</sup> exchangers and Na<sup>+</sup>/K<sup>+</sup>-ATPase [2].

<sup>23</sup>Na nucleus has spin 3/2 and 100% natural abundance, therefore this nucleus can be detected by nuclear magnetic resonance (NMR) methods [3].

Sodium magnetic resonance imaging (MRI) is a quantitative *in vivo* method allowing to estimate cell integrity and tissue viability. Examples of clinical application include

Corresponding Author:  
Elnur G. Sadykhov  
forward1292@gmail.com

Received: 17 January 2018  
Accepted: 25 March 2018  
Published: 17 April 2018

Publishing services provided by  
Knowledge E

© Sadykhov E.G. et al. This article is distributed under the terms of the [Creative Commons Attribution License](#), which permits unrestricted use and redistribution provided that the original author and source are credited.

Selection and Peer-review under the responsibility of the PhysBioSymp17 Conference Committee.

## OPEN ACCESS

cerebral stroke, brain and breast tumors, cardiac infarction, Alzheimer's disease, multiple sclerosis, hypertension, osteoarthritis, renal failure. The use of  $^{23}\text{Na}$  MRI in conjunction with  $^1\text{H}$  MR techniques will help the diagnosis, prognosis of diseases and treatment outcomes.

The problem considered by our group in this work was to determine the sensitivity of  $^{23}\text{Na}$  MR spectroscopy (MRS), MRI methods to different  $^{23}\text{Na}$  concentrations and make an optimal protocol of  $^{23}\text{Na}$  MR study for small animals (rat, mouse) using 3D FLASH (fast low angle shot) pulse sequence on 7T MR scanner Bruker Biospec 70/30 USR.

We also aimed at differentiating sample states based on  $^{23}\text{Na}$   $T_1$  and  $T_2$  relaxometry. The relaxometry parameters may serve as endogenous markers of underlying physiology. For instance, E. Staroswiecki et al. [4] showed an increase in the  $^{23}\text{Na}$   $T_2$  within tumors in the human breast at 3 T. Another example is the work made by M. Lupu et al. at 4.7 T [5] where  $^{23}\text{Na}$   $T_2$ - relaxometry was performed on mouse liver, revealing differences between normal and Hepatocellular Carcinoma bearing liver. C. Thomas et al. [6] carried out cisplatin treatment monitoring by  $^{23}\text{Na}$  MRI relaxometry at 4.7 T in colorectal tumors implanted on mice.

## 2. Materials and methods

The experiment was carried out on 7T MR scanner Bruker Biospec 70/30 USR with maximum gradient strength 105 mT/m using ParaVision 5.0 software. Protocol testing was implemented *in vitro* on the phantoms (plastic vials with the volume 14 ml) which comprised different concentrations of NaCl and gelatine (Table 1). Gelatine was chosen as gel forming substance in order to mimic biological semi-solid tissues. Distilled water was used as a solvent in all cases.

TABLE 1:  $^{23}\text{Na}$  peak integral and height ratios for different concentrations of NaCl and gelatine.

Phantoms	Integral ratio	Height ratio
0.05, 0.1, 0.14, 5.3 M NaCl	1:2.1:2.8:95	1:2:2.8:92
0.05, 0.1, 0.14 M NaCl + 1% gelatine	1:2.1:3.2	1:1.6:3.1
0.05, 0.1, 0.14 M NaCl + 2% gelatine	1:1.9:2.5	1:1.7:2.3
0.05, 0.1, 0.14, 5.3 M NaCl + 4% gelatine	1:2.1:2.8:114.2	1:2:2.6:98.2

The protocol of study comprised two parts: proton and sodium. The first one consisted of automatic shimming (global) and localizing. These 2 steps were realized with

$^1\text{H}$  Bruker transceiver volume radiofrequency (RF) coil. The  $^{23}\text{Na}$  part included determination of 3D FLASH optimal parameters. Sodium nuclei excitation and signal reception were implemented by means of a RF surface coil with 2 cm internal diameter. The  $^{23}\text{Na}$  coil is a modified proprietary transceiver coil (Figure 1) originally tuned to the  $^{13}\text{C}$  frequency. The coil was placed too close on the phantoms.



**Figure 1:** View of the  $^{23}\text{Na}$  surface coil.

The  $^{23}\text{Na}$  resonance frequency  $\approx 79.57$  MHz was defined by recording  $^{23}\text{Na}$  MR spectra in TopSpin 2.0 software and set in ParaVision 5.0 software for obtaining  $^{23}\text{Na}$  MR images. The free induction decay (FID) signal for  $^{23}\text{Na}$  MRS was acquired with a  $90^\circ$  single block pulse of duration  $90 \mu\text{s}$  and power  $\approx 1.6$  W. The other parameters were: repetition time (TR) = 350 ms, number of scans (NS) = 2, size of FID = 2048 points, zero filling factor = 2, sweep width (SW) = 5 kHz, acquisition time (TA) = 0.7 s. RF pulse calibration was implemented by changing the pulse duration gradually until the  $^{23}\text{Na}$  peak went through a null indicating a  $180^\circ$  pulse. The signal-to-noise ratios (SNRs) of  $^{23}\text{Na}$  spectra were calculated using the algorithm embedded in TopSpin 2.0 software.

We used RARE-VTR (rapid acquisition with relaxation enhancement with variable repetition time) and MSME (multi slice multi echo) pulse sequences to measure  $^{23}\text{Na}$   $T_1$  and  $T_2$  values respectively.  $T_1$ -relaxometry was carried out with 16 values of TR (from 10 to 350 ms), TE = 6 ms, NS was taken 4 for saturated NaCl, 16 for 0.14 M, 32 for 0.1 and 0.05 M NaCl.  $T_2$ -relaxometry was conducted with 25 values of TE (from minimum 5.74 to 143.5 ms), TR = 350 ms, NS = 4 for saturated NaCl, 32 for 0.14 M, 64 for 0.1 M and 128 for 0.05 M NaCl. Both types of measurement comprised block excitation  $90^\circ$  and refocusing  $180^\circ$  RF pulses of the same duration ( $90 \mu\text{s}$ ) and different power (1.6 and 6.3 W respectively).

$^{23}\text{Na}$  MR images were acquired using 3D FLASH pulse sequence with the optimal parameters. The quality of obtained  $^{23}\text{Na}$  images was estimated in terms of SNR using ImageJ 1.51j8 software [7]. According to the formula (A11) in [8], SNR was defined as  $0.66 \cdot S/N$  where S is a mean value in the region-of-interest (ROI) defined in the upper part of the axial slice of the phantom and N is a standard deviation in the ROI defined outside the phantom.

### 3. Results

The  $^{23}\text{Na}$  MR spectra of the prepared phantoms were obtained.  $^{23}\text{Na}$  MRS was conducted with NS = 2 enough to get high SNR. In case of scanning the phantom with minimum NaCl concentration (50 mM), the SNR of the spectrum was  $\approx 80$ . It allowed to acquire  $^{23}\text{Na}$  spectra quite fast (TA = 0.7 s). The calculated linewidth of the obtained  $^{23}\text{Na}$  peaks was in the range from 35 to 45 Hz (line broadening was taken 10 Hz), what validated the good shimming. In order to check the capability to recognize changes in  $^{23}\text{Na}$  concentration of the objects scanned, the integral and height ratios for  $^{23}\text{Na}$  peaks were calculated (Table 1). It can be seen that  $^{23}\text{Na}$  MRS is able to differentiate  $^{23}\text{Na}$  concentrations. Examples of  $^{23}\text{Na}$  MRS are shown in Figure 2.

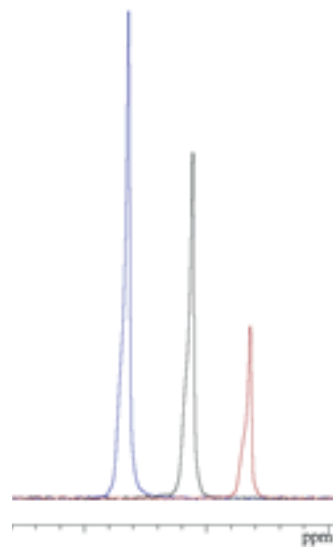


**Figure 2:**  $^{23}\text{Na}$  MR spectra of 0.05 M (red), 0.1 M (black) and 0.14 M (blue) NaCl solutions; the spectra are shifted for clarity.

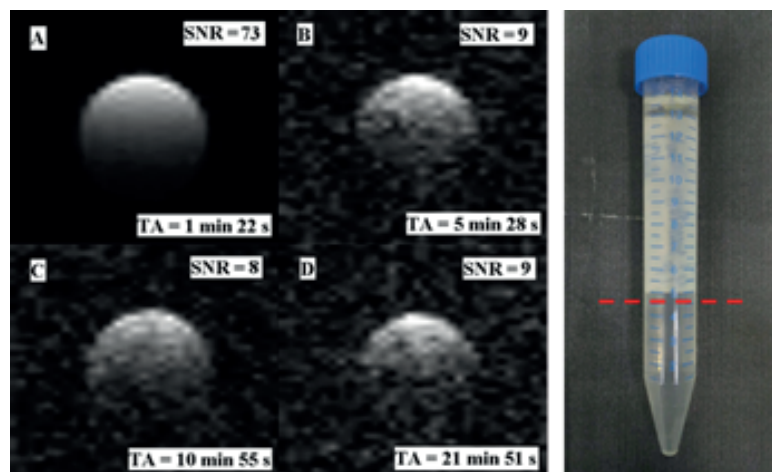
The optimization of main scanning parameters was made taking into account the size of the  $^{23}\text{Na}$  surface coil and the opportunities of 3D FLASH method. In order to achieve high SNR, the field of view (FOV) was set larger than coil dimensions. The matrix size was selected to achieve good spatial resolution and acceptable acquisition time (<25 min for minimum NaCl concentration). The large SW (70 kHz) and short RF pulse were taken to set small TE to attain high intensity  $^{23}\text{Na}$  MR signal. To achieve the good quality of  $^{23}\text{Na}$  images the RF pulse was chosen non-rectangular. The pulse power was determined based on pulse duration and FA value. For the purpose of finding the optimal TR, the  $^{23}\text{Na}$  MRI of the saturated NaCl phantom was performed using different TRs (160, 80, 40, 20 and 10 ms), and the corresponding SNRs were calculated (Table 2). Based on the TR and  $T_1$  values, the FA was taken equal to Ernst angle [9].

TABLE 2: The  $^{23}\text{Na}$  3D FLASH MRI SNRs for different TRs and fixed TA. The sample is saturated NaCl solution.

No.	TR, ms	NS	TA	SNR
1	160	1	1 min 22 s	20
2	80	2		27
3	40	4		39
4	20	8		50
5	10	16		71

The following parameters were chosen for 3D FLASH  $^{23}\text{Na}$  MRI as optimum: TR/TE = 10/3.8 ms, FA = 30°, FOV = 6×4×4 cm, MTX = 64×64×8, Gaussian pulse of duration 270 μs and power ≈100 mW, SW = 70 kHz. In order to obtain acceptable quality  $^{23}\text{Na}$  MR images (SNR≥5), the parameter TA was different for each sample regardless of the gelatine concentration: 1 min 22 s for 5.3 M NaCl, 5 min 28 s for 0.14 M NaCl, 10 min 55 s for 0.1 M NaCl and 21 min 51 s for 0.05 M NaCl. The MR scanning was performed in the axial projection.

The SNRs for  $^{23}\text{Na}$  images (examples are shown in Figure 3) are given in the Table 3. It is seen from Table 3 that even for small NaCl concentrations the achieved SNR≥5. The highest  $^{23}\text{Na}$  image signal intensity is observed in the upper part of phantoms since the surface coil produces the non-uniform RF magnetic field.



**Figure 3:**  $^{23}\text{Na}$  MR images of phantoms (axial slices). A – 5.3 M NaCl + 4% gelatine; B – 0.14 M NaCl + 4% gelatine; C – 0.1 M NaCl + 4% gelatine; D – 0.05 M NaCl + 4% gelatine. On the right is the view of NaCl phantom. The red dashed line through the phantom designates the axial projection.

To determine the sensitivity of  $^{23}\text{Na}$  3D FLASH MRI method with optimized parameters, the mass of  $^{23}\text{Na}$  in each voxel for the minimum NaCl concentration was calculated. The 0.05 M  $^{23}\text{Na}$  concentration is equivalent to ≈3.4 μg of  $^{23}\text{Na}$  per used voxel size of 2.93 mm<sup>3</sup>.

TABLE 3:  $^{23}\text{Na}$  3D FLASH MRI SNR,  $T_1$  and  $T_2$  values of  $^{23}\text{Na}$  and their standard deviations for different concentrations of NaCl and gelatine (gel.).

No.	Phantom		SNR	$T_1$ , ms	$T_2$ , ms
	C(NaCl), M	C(gel.), %			
1	5.3	0	71	48.6±1.4	35.3±0.3
2	0.14	0	9	88.7±5.1	56.7±1.7
3	0.1	0	10	87.7±3.7	54.7±1.2
4	0.05	0	7	71.4±7.8	n/a
5	0.14	1	8	66.7±6.2	49.2±1.3
6	0.1	1	9	66.5±2.9	55.1±1.2
7	0.05	1	5	65.5±3.5	n/a
8	0.14	2	10	64.6±3.2	53.3±1.4
9	0.1	2	9	68.6±5.5	54.4±0.9
10	0.05	2	6	64.1±4.8	n/a
11	5.3	4	73	35.8±0.6	27.9±0.4
12	0.14	4	9	59.2±2.8	46.6±1.0
13	0.1	4	8	56.4±4.3	48.1±1.6
14	0.05	4	9	55.3±5.3	n/a

The results for  $T_1$ - and  $T_2$ -relaxometry are shown in the Table 3. Considering the samples No. 1–4 and 11–14 from the Table 3, it's noticeable that the  $T_1$  and  $T_2$  values in case of saturated NaCl solution are less than for more dilute NaCl solutions. Addition of 4% gelatine to saturated NaCl results in reduction of  $T_1$  and  $T_2$ . The decrease of  $T_1$  is observed for small NaCl concentrations when augmenting the gelatine concentration but there is no sustained change in  $T_2$ . The measurements of  $T_2$  for 50 mM NaCl phantoms weren't reliable because of the low SNR (<3) therefore corresponding results aren't specified.

## 4. Discussion

It can be seen from Table 1 that integral ratios are in good concordance with NaCl concentration ratio which is 1:2:2.8:106, as expected. This result shows the good sensitivity of  $^{23}\text{Na}$  MRS to discriminate different  $^{23}\text{Na}$  concentrations.

Based on the acquired  $^{23}\text{Na}$  images we can claim that the used 3D FLASH method is sensitive to minimum  $\text{Na}^+$  concentration (50 mM) considered. According to [10], the

average tissue sodium concentration measured in brain is  $\approx 45$  mM what determines the choice of minimum NaCl concentration in our study.

Our  $^{23}\text{Na}$   $T_1$ - and  $T_2$ -relaxometry measurements showed the opportunity to discriminate liquid and solid states of the objects scanned: the more solid the sample, the lower  $T_1$  and  $T_2$ . However our measurements didn't reveal any regularity when analyzing  $T_1$  and  $T_2$  for the phantoms with the biological  $\text{Na}^+$  concentrations (0.14, 0.1, 0.05 M) within the same gelatine concentration. This may be a problem when differentiating  $^{23}\text{Na}$  concentrations in *in vivo*  $^{23}\text{Na}$  MR experiments.

Furthermore, it is worth noting that  $^{23}\text{Na}$  nucleus has the quadrupole moment, therefore  $^{23}\text{Na}$  experiences a biexponential  $T_2$  relaxation in biological tissues. It is known that a short  $T_2$  component  $T_{2,fast} < 3$  ms gives 60% of the MR signal, while a long  $T_2$  component  $T_{2,slow} > 20$  ms corresponds to 40% of the signal [11]. Since the minimum TE we used in  $T_2$ -relaxometry was quite big (5.74 ms), we can suppose that we measured only long  $T_2$  component. The use of the advanced technique such as ultrashort echo time (UTE) pulse sequence can allow to measure short  $T_2$  component as well if there are no technical constraints of MR hardware.

## 5. Conclusion

We conducted the MR phantom experiment to show the capability to detect different  $^{23}\text{Na}$  concentrations within the range of biological values. Our study demonstrated the high sensitivity of single-pulse  $^{23}\text{Na}$  MRS on 7T MR scanner Bruker Biospec 70/30 USR and the ability of  $^{23}\text{Na}$  MR relaxometry to distinguish the samples with different density that can be useful in differentiating normal and injured tissues. We optimized the conventional MR scanning 3D FLASH method for  $^{23}\text{Na}$  signal detection at 7 T and developed the MRI protocol for small animal  $^{23}\text{Na}$  *in vivo* visualization.

## Acknowledgements

This work was carried out in the Centre for Collective Usage "Biospectromotography" supported by the Faculty of Fundamental Medicine of Lomonosov Moscow State University, Moscow, Russia.

## References

- [1] M. Burnier, *Sodium in Health and Disease*. New York: Informa Healthcare USA, Inc., 2008.
- [2] E. Murphy and D. Eisner, "Regulation of intracellular and mitochondrial sodium in health and disease," *Circ. Res.*, vol. 104, pp. 292-303, 2009.
- [3] G. Madelin et al., "Sodium MRI: Methods and applications," *Prog. Nucl. Magn. Reson. Spectrosc.*, vol. 79, pp. 14-47, 2014.
- [4] E. Staroswiecki et al., "In Vivo Sodium Imaging and Relaxometry of the Breast at 3T," in *Proc. Intl. Soc. Mag. Reson. Med.* 17, 2009, p. 2129.
- [5] M. Lupu et al., "IN VIVO SODIUM MRI RELAXOMETRY OF NORMAL AND PATHOLOGICAL MOUSE LIVER AT 4.7 T," in *Proc. Intl. Soc. Mag. Reson. Med.* 15, 2007, p. 1329.
- [6] C. Thomas et al., "Cisplatin treatment monitoring by sodium MRI relaxometry at 4.7 T in colorectal tumors implanted on mice," in *Proc. Intl. Soc. Mag. Reson. Med.* 16, 2008, p. 2795.
- [7] G. Schneider, W. Rasband, and K. Eliceiri, "NIH Image to ImageJ: 25 years of image analysis," *Nat. Methods*, vol. 9, pp. 671-675, 2012.
- [8] O. Dietrich et al., "Measurement of Signal-to-Noise Ratios in MR Images: Influence of Multichannel Coils, Parallel Imaging, and Reconstruction Filters," *J. Magn. Reson. Imaging*, vol. 26, pp. 375-385, 2007.
- [9] R. Ernst and W. Anderson, "Application of Fourier transform spectroscopy to magnetic resonance," *Rev Sci Instrum*, vol. 37, pp. 93-102, 1966.
- [10] J. Christensen et al., "Quantitative tissue sodium concentration mapping of normal rat brain," *Magn. Reson. Med.*, vol. 36, pp. 83-89, 1996.
- [11] Ouwerkerk R., "Sodium MRI," *Methods Mol. Biol.*, vol. 711, pp. 175-201, 2011.